

SINGLE-PASS NYSTRÖM APPROXIMATION IN MIXED PRECISION

ERIN CARSON* AND IEVA DAUŽICKAITĖ*

Abstract. Low rank matrix approximations appear in a number of scientific computing applications. We consider the Nyström method for approximating a positive semidefinite matrix A . The computational cost of its single-pass version can be decreased by running it in mixed precision, where the expensive products with A are computed in a lower than the working precision. We bound the extra finite precision error which is compared to the error of the Nyström approximation in exact arithmetic and identify when the approximation quality is not affected by the low precision computations. The mixed precision Nyström method can be used to inexpensively construct a limited memory preconditioner for the conjugate gradient method. We bound the condition number of the preconditioned coefficient matrix, and experimentally show that such preconditioner can be effective.

Key words. mixed precision, Nyström method, randomization, preconditioning, conjugate gradient

AMS subject classifications. 65F08, 65F10, 65F50, 65G50, 65Y99

1. Introduction. We consider the construction of a rank k approximation A_N to a positive semidefinite matrix $A \in \mathbb{R}^{n \times n}$ of the form

$$A_N = (AX)(X^T AX)^\dagger (AX)^T, \quad (1.1)$$

where $X \in \mathbb{R}^{n \times k}$ is a sampling matrix and \dagger denotes the Moore-Penrose pseudoinverse. When the matrix A is symmetric positive semidefinite, then a high quality approximation can be obtained using the Nyström method as shown theoretically and experimentally in [13]. The Nyström method, a randomised approach, arises in two forms based on column-sampling and general random projections. The column-sampling approach is often analysed and used in machine learning setting [32, 9] and the general projection version has been explored for, e.g., approximating matrices in a streaming model [28, 29] and preconditioning linear systems of equations [3, 6, 10]. In general, randomised methods are powerful tools for obtaining low-rank matrix approximations and are discussed in extensive reviews [15, 21, 22].

In this paper, we focus on the projection based approach, and the case when products with A are very expensive and thus are the bottlenecks of the randomised methods. Such a setting motivates using single-pass versions that require only one matrix-matrix product with A to reduce the overall cost. These are also employed in the streaming model, because A can only be accessed once.

The increasing commercial availability of hardware with low and mixed precision capabilities has inspired much recent work in developing mixed precision algorithms that can exploit this hardware to improve performance [1]. For instance, the latest NVIDIA H100 GPUs offer IEEE double (64 bit), IEEE single (32 bit), IEEE half (16 bit), and even quarter (8 bit) floating point storage and computation. When using specialized tensor core instructions, quarter precision can offer up to 4 petaflops/s and half precision (fp16) up to 2 petaflops/s performance on a single H100 GPU,

*Faculty of Mathematics and Physics, Charles University. Both authors were supported by Charles University PRIMUS project no. PRIMUS/19/SCI/11 and by the Exascale Computing Project (17-SC-20-SC), a collaborative effort of the U.S. Department of Energy Office of Science and the National Nuclear Security Administration. The first author was additionally supported by Charles University Research program no. UNCE/SCI/023.

compared to 60 teraflops/s for double precision (fp64) [4]. See Table 1.1 for the unit roundoff and range for some IEEE floating-point arithmetics.

| Arithmetic | u | Range | | |
|---------------|--|-------------------------|-------------------------|------------------------|
| | | x_{min}^s | x_{min} | x_{max} |
| fp16 (half) | $2^{-11} \approx 4.88 \times 10^{-4}$ | 5.96×10^{-8} | 6.10×10^{-5} | 6.55×10^4 |
| fp32 (single) | $2^{-24} \approx 5.96 \times 10^{-8}$ | 1.40×10^{-45} | 1.18×10^{-38} | 3.40×10^{38} |
| fp64 (double) | $2^{-53} \approx 1.11 \times 10^{-16}$ | 4.94×10^{-324} | 2.22×10^{-308} | 1.80×10^{308} |

Table 1.1: Unit roundoff u for IEEE floating point arithmetics and the smallest positive subnormal number x_{min}^s , smallest positive number x_{min} , and the largest positive number x_{max} .

Given that in our particular setting, the matrix-matrix products with A are overwhelmingly the dominant cost, we thus seek to further reduce this cost through the use of low precision. We develop a mixed precision single-pass Nyström approach in which storage of and computation with A is performed at a precision lower than the working precision.

The natural question to ask is how does using the lower precision affect the quality of the approximation. We prove a bound on the error of $\|A - \hat{A}_N\|_2$, where \hat{A}_N is the approximation computed by the mixed precision algorithm. Intuitively, this can be bounded in terms of the deviation of the exact (infinite precision) Nyström approximation A_N from A and the deviation of \hat{A}_N from A_N . Our results can thus be used to determine how low a precision can safely be used so that the error of the exact Nyström approximation remains dominant.

We also consider the impact of the low-precision computations in preconditioning. Our focus is on limited memory preconditioners that can be constructed using the Nyström approximation and have been used in [6, 10]. We extend the bounds on the condition number of the preconditioned system given in [10] to account for finite precision error.

The paper is structured as follows. In Section 2, we discuss known bounds for the exact single-pass Nyström approximation, and derive and analyze a mixed precision variant. Then in Section 3 we consider the application of our mixed precision approach to constructing limited memory preconditioners. Numerical examples are presented in Section 4 and we conclude the paper in Section 5.

2. Nyström approximation. The approximation A_N in (1.1) can be written using an orthogonal projector $P_{A^{1/2}X} = (A^{1/2}X)(X^TAX)^\dagger(A^{1/2}X)^T$ as $A_N = A^{1/2}P_{A^{1/2}X}A^{1/2}$ and thus the quality of the approximation depends on the range of X . This motivates using X that depend on A , for example, $X = AG$, where G is a random test matrix. Such an approach may be infeasible when the products with A are expensive or in the streaming model, and thus we do not consider it in this paper.

Structured sampling matrices that are suitable for fast products with A can be used and experiments show that they can give a good quality approximation; see, for example, Section 9 in [22]. However most of the theoretical results are for Gaussian matrices. We thus consider the orthonormal model, where the test matrix X can be chosen to be the Q factor from the QR decomposition of a Gaussian matrix G . The resulting approximation is the same as when using G in exact arithmetic, but orthogonal matrices are preferred for stability in finite precision when k is large [28]. Algorithm 2.1 is based on the stable implementation that appears in [28] (although

we note that there is no specification of precision in [28]).

Various deterministic and probabilistic bounds for the exact approximation error

$$E = A - A_N \tag{2.1}$$

appear in the literature, e.g., [13, 28, 10]. Let $\lambda_1 \geq \lambda_2 \geq \dots \geq \lambda_n$ be the eigenvalues of A . Gittens and Mahoney provide a deterministic bound for $\|E\|_2$ that is a sum of the smallest possible error λ_{k+1} and a term that depends on $\lambda_{k+1}, \lambda_{k+2}, \dots, \lambda_n$ and how well the sketching matrix approximates the eigenspace of A (Theorem 2 in [13]). The deterministic bounds are pessimistic and the error estimate can be improved considering the expected error or bounds that hold with high probability [12]. For example, a recent result by [10] bounds the expected exact approximation error of a rank $k \geq 4$ approximation A_N obtained by Algorithm 2.1 by

$$\mathbb{E} \|A - A_N\|_2 \leq \min_{2 \leq p \leq k-2} \left(\left(1 + \frac{2(k-p)}{p-1} \right) \lambda_{k-p+1} + \frac{2e^2 k}{p^2 - 1} \sum_{j=k-p+1}^n \lambda_j \right), \tag{2.2}$$

where $\lambda_i \geq \lambda_{i+1}$ are eigenvalues of A and e is the exponential constant.

The finite precision error for randomised methods is usually not analysed with the notable exception of [25] who showed that a stabilised generalised Nyström approximation is stable. In the following subsection, we introduce a mixed precision variant of the stabilised single-pass Nyström approximation and analyze the error in finite precision.

Algorithm 2.1 Stabilised single-pass Nyström approximation for symmetric positive semidefinite A in precisions u and u_p

Input: symmetric positive semidefinite matrix $A \in \mathbb{R}^{n \times n}$ stored in precision u_p , a target rank k , an oversampling parameter l

Output: $U \in \mathbb{R}^{n \times k}$ with orthonormal columns approximating eigenvectors of A , and diagonal $\Theta \in \mathbb{R}^{k \times k}$ with approximations to the largest k eigenvalues of A on the diagonal

- | | |
|--|--|
| 1: $G = \text{randn}(n, k + l)$ | $\triangleright u$ |
| 2: $[Q, \sim] = \text{qr}(G, 0)$ | $\triangleright u$ |
| 3: $Y = AQ$ | \triangleright compute in u_p , store in u |
| 4: Compute a shift ν : $\nu = \epsilon * \text{norm}(Y, 'fro')$ | $\triangleright u$; $\epsilon = 2u_p$ |
| 5: Shift Y : $Y_\nu = Y + \nu Q$ | $\triangleright u$ |
| 6: $B = Q^T Y_\nu$ | $\triangleright u$ |
| 7: Cholesky: $C = \text{chol}((B + B')/2)$ | $\triangleright u$ |
| 8: Solve $F = Y_\nu / C$ | $\triangleright u$ |
| 9: Form SVD $[U, \Sigma, \sim] = \text{svd}(F, 0)$ | $\triangleright u$ |
| 10: Remove oversampled columns/rows: $U = U(:, 1 : k)$, $\Sigma = \Sigma(1 : k, 1 : k)$ | |
| 11: Remove the shift: $\Theta = \text{max}(0, \Sigma^2 - \nu I)$ | $\triangleright u$ |
-

2.1. Finite precision error. We consider the case where the expensive product with A is performed in precision u_p , which is assumed to be a lower precision than the working precision u used in other steps of the algorithm, i.e., $u \ll u_p$. Note that since this is the only time A is accessed, we also store A in precision u_p . We assume all other quantities are stored in precision u . The computed approximation is denoted

\widehat{A}_N and the finite precision error is denoted

$$\mathcal{E} = A_N - \widehat{A}_N. \quad (2.3)$$

We aim to bound the L_2 norm of \mathcal{E} in order to give a bound on the total error of the approximation via

$$\|A - \widehat{A}_N\|_2 = \|A - A_N + A_N - \widehat{A}_N\|_2 \leq \|E\|_2 + \|\mathcal{E}\|_2.$$

We use a standard model of floating point arithmetic; see, e.g., [16, Section 2.2]. We assume in our analysis that no overflow or underflow occurs, although we note that this can become increasingly common when very low precisions are used. Following [16], we define

$$\gamma_n^{(p)} = \frac{nu_p}{1 - nu_p}, \quad \widetilde{\gamma}_n^{(p)} = \frac{cnu_p}{1 - cnu_p},$$

where c is a small constant independent of n . For a nonsingular matrix A , $\kappa(A)$ will be used to denote the 2-norm condition number, i.e., $\kappa(A) = \|A^{-1}\|_2 \|A\|_2$.

Our main result in this section is the following theorem.

THEOREM 2.1. *Let $A \in \mathbb{R}^{n \times n}$ be a symmetric positive semidefinite matrix stored in precision u_p , and \widehat{A}_N be its approximation computed by Algorithm 2.1 using precision u_p in step 3 and precision $u \ll u_p$ in other steps. Then with high probability the approximation error is bounded by*

$$\|A - \widehat{A}_N\|_2 \leq \|A - A_N\|_2 + n^{3/2} \widetilde{\gamma}_n^{(p)} \|A\|_2.$$

Proof. We assume that rounding errors from all computations performed in precision $u \ll u_p$ are insignificant compared to those performed in precision u_p and can thus be ignored. This assumption will not change the main conclusions but will simplify the analysis considerably. We thus assume that Q in step 2 of Algorithm 2.1 is orthogonal and using standard results in [16] (eq. 3.13) in step 3 we compute

$$\widehat{Y} = AQ + \Delta,$$

where

$$\|\Delta\|_2 \leq \sqrt{n} \widetilde{\gamma}_n^{(p)} \|A\|_2. \quad (2.4)$$

Then the computed approximation is

$$\begin{aligned} \widehat{A}_N &= (AQ + \Delta) \left(Q^T AQ + \frac{1}{2}(Q^T \Delta + \Delta^T Q) \right)^\dagger (AQ + \Delta)^T \\ &= (AQ + \Delta) \left(Q^T AQ + \frac{1}{2}(Q^T \Delta + \Delta^T Q) \right)^{-1} (AQ + \Delta)^T, \end{aligned}$$

because we ensure that $Q^T AQ + \frac{1}{2}(Q^T \Delta + \Delta^T Q)$ is positive definite for the Cholesky factorization. We denote

$$\widetilde{\Delta} = \frac{1}{2}(Q^T \Delta + \Delta^T Q)$$

and approximate the inverse to the first order in $\tilde{\Delta}$, that is,

$$\begin{aligned} (Q^T A Q + \tilde{\Delta})^{-1} &\approx \left(I - (Q^T A Q)^{-1} \tilde{\Delta} \right) (Q^T A Q)^{-1} \\ &= (Q^T A Q)^{-1} - (Q^T A Q)^{-1} \tilde{\Delta} (Q^T A Q)^{-1}. \end{aligned}$$

Then

$$\hat{A}_N \approx (A Q + \Delta)(Q^T A Q)^{-1}(A Q + \Delta)^T - (A Q + \Delta)(Q^T A Q)^{-1} \tilde{\Delta} (Q^T A Q)^{-1} (A Q + \Delta)^T.$$

The first order in Δ approximation is

$$\begin{aligned} \hat{A}_N &\approx A_N + A Q (Q^T A Q)^{-1} \Delta^T + \Delta (Q^T A Q)^{-1} (A Q)^T \\ &\quad - \frac{1}{2} A Q (Q^T A Q)^{-1} Q^T \Delta (Q^T A Q)^{-1} (A Q)^T \\ &\quad - \frac{1}{2} A Q (Q^T A Q)^{-1} \Delta^T Q (Q^T A Q)^{-1} (A Q)^T. \end{aligned} \quad (2.5)$$

From the above, we can bound

$$\|\hat{A}_N - A_N\|_2 \lesssim (2\|A Q (Q^T A Q)^{-1}\|_2 + \|A Q (Q^T A Q)^{-1}\|_2^2) \|\Delta\|_2.$$

Our task is thus to bound the norm of $A Q (Q^T A Q)^{-1}$. This can be done following the approach in Lemma 3.2 of [25]. Employ the SVD of $A Q = U \Sigma V^T$, then

$$\begin{aligned} \|A Q (Q^T A Q)^{-1}\|_2 &= \|U \Sigma V^T (Q^T U \Sigma V^T)^{-1}\|_2 \\ &= \|\Sigma V^T V (Q^T U \Sigma)^{-1}\|_2 \\ &= \|(Q^T U)^\dagger (Q^T U) \Sigma (Q^T U \Sigma)^{-1}\|_2 \\ &= \|(Q^T U)^\dagger\|_2. \end{aligned}$$

To bound $\|(Q^T U)^\dagger\|_2$, we consider $G = Q R$, where G is the Gaussian matrix computed in step 1 of Algorithm 2.1 and factors Q and R are computed in step 2. Then

$$Q^T U = R^{-T} G^T U.$$

R has a full column rank and $G^T U$ has a full row rank with probability one, thus

$$(R^{-T} G^T U)^\dagger = (G^T U)^\dagger R^T.$$

Matrix $G^T U$ is Gaussian, because G is Gaussian and U has orthogonal columns. Rudelson and Vershynin showed that the smallest singular value of a $k \times k$ Gaussian matrix is of order $1/\sqrt{k}$ with high probability [26], thus

$$\|(G^T U)^\dagger\|_2 \leq c_1 \sqrt{k} \quad (2.6)$$

with high probability for some constant c_1 . $\|R\|_2 = \|G\|_2$ is bounded using Theorem 2.13 of Davidson and Szarek [7], that is,

$$\|G\|_2 \leq \sqrt{n} + \sqrt{k} + t \quad (2.7)$$

with high probability for some $t > 0$. Then (2.6) and (2.7) give

$$\|A Q (Q^T A Q)^{-1}\|_2 \leq \tilde{c} \sqrt{n}$$

with high probability for a constant \tilde{c} independent of n . Combining with (2.5) and (2.4) gives

$$\begin{aligned}\|A - \hat{A}_N\|_2 &\leq \|A - A_N\|_2 + (2\tilde{c}\sqrt{n} + \tilde{c}^2 n)\|\Delta\|_2 \\ &\leq \|A - A_N\|_2 + n^{3/2}\tilde{\gamma}_n^{(p)}\|A\|_2.\end{aligned}$$

□

The structure of the bound for the total error, that is, it being a sum of the exact approximation error and an additional term for the finite precision error, gives us insight into when setting u_p to lower than the working precision may be appropriate. The finite precision error may be essentially ignored if $n^{3/2}\tilde{\gamma}_n^{(p)}\|A\|_2 \lesssim \|A - A_N\|_2$. The exact approximation error $\|A - A_N\|_2$ is expected to decrease when the rank k of the approximation is increased, hence the effect of the lower precision error may be important for large rank approximations.

We can roughly estimate when $\|E\|_2$ and $\|\mathcal{E}\|_2$ become of the same order. When A_N is a rank k approximation then $\|E\|_2$ depends on the eigenvalues $\lambda_{k+1} \geq \lambda_{k+2} \geq \dots \geq \lambda_n$, and we assume that $\|E\|_2$ is dominated by λ_{k+1} . In practice we observe that $\|AQ(Q^T AQ)^{-1}\|_2 = O(1)$ and the finite precision error $\|\mathcal{E}\|_2$ is dominated by $\tilde{\gamma}_n^{(p)}\|A\|_2$, which we approximate by $nu_p\|A\|_2 = nu_p\lambda_{max}$ and further simplify to $\sqrt{n}u_p\lambda_{max}$ using the rule of thumb that n can be replaced by \sqrt{n} [16]. The finite precision error of a rank k approximation \hat{A}_N can thus be expected to affect the approximation quality when

$$\frac{\lambda_{k+1}}{\lambda_{max}} \approx \sqrt{n}u_p. \quad (2.8)$$

3. Preconditioning. We now consider an important area where low-rank matrix approximations are used, namely preconditioning iterative solvers. A useful preconditioner has to be inexpensive to construct and apply while accelerating the convergence of an iterative solver.

Let $A \in \mathbb{R}^{n \times n}$ be a symmetric positive semidefinite matrix, so that it can be approximated via the Nystrom method, and consider a system of linear equations of the form

$$(A + \mu I)x = b, \quad (3.1)$$

where $\mu \geq 0$ so that $A + \mu I$ is positive definite, $I \in \mathbb{R}^{n \times n}$ is an identity matrix, and $x, b \in \mathbb{R}^n$. Preconditioned conjugate gradient (PCG) is a popular method for systems with symmetric positive definite coefficient matrices; see, e.g., [27].

We focus on the case where A has rapidly decreasing eigenvalues or a cluster of large eigenvalues; notice that the spectrum of $A + \mu I$ has the same structure. In such settings, finite precision PCG convergence can be slow [5] and removing the largest eigenvalues with a preconditioner can accelerate convergence. This can be achieved using a spectral limited memory preconditioner (LMP), defined as

$$P = I - UU^T + \frac{1}{\alpha + \mu}U(\Theta + \mu I)U^T, \quad (3.2)$$

$$P^{-1} = I - UU^T + (\alpha + \mu)U(\Theta + \mu I)^{-1}U^T, \quad (3.3)$$

where the columns of $U \in \mathbb{R}^{n \times k}$ are approximate eigenvectors of A and $U^T U = I$, Θ is diagonal with approximations to the eigenvalues of A , and $\alpha \geq 0$.

The expression (3.3) is an instance of a general class of limited memory preconditioners studied in [31, 14, 30] and used in data assimilation [24, 23, 20]. Algorithm 2.1 returns an eigendecomposition of A_N and thus can be used to construct (3.2). The randomised version of the preconditioner is mentioned in [22] (section 17) and is analysed in [10], where it is called a randomised Nyström preconditioner. It is also explored in a data assimilation setting under the name randomised LMP in [6].

It is easy to show that if (3.3) is constructed using exact eigenpairs, then the eigenvalues used to construct the preconditioner are mapped to $\alpha + \mu$ and other eigenvalues remain unchanged. This cannot be guaranteed when constructing the preconditioner with approximations to the eigenpairs, but a study of the eigenvalues of the preconditioned matrix when (3.2) is constructed with eigenvalues of $A + tE$, where $\|E\|_2 = 1$, $t \in \mathbb{R}$ is small, and $\mu = 0$, in [11] by Giraud and Gratton show that if the preconditioner is constructed using high quality approximations of not clustered or not small isolated eigenpairs, then the eigenvalues in the inexact case will be close to the exact ones.

If we have information on existing eigenvalue clusters of A , we may use it to choose α and thus send the largest eigenvalues close to an already existing cluster. Martinsson and Tropp in [22] suggest setting $\alpha = \lambda_k$, where λ_k is the smallest nonzero eigenvalue of A_N . This is done in the hope that the spectrum of $P^{-1}(A + \mu I)$ is then more clustered compared to A , and the condition number is reduced. Note that the condition number alone does not determine the PCG convergence behaviour and the same holds for the number of clusters of eigenvalues; see [5] for detailed commentary. A small condition number however can indicate fast convergence. In the following section, we consider the resulting condition number when the mixed precision Nyström approximation in Algorithm 2.1 is used to construct the preconditioner.

3.1. Bound on condition number of preconditioned coefficient matrix.

The work in [10] provides bounds for the condition number of the preconditioned coefficient matrix in exact precision. We extend them to include the finite precision error in the preconditioner

$$\hat{P}^{-1} = I - \hat{U}\hat{U}^T + (\hat{\lambda}_k + \mu)\hat{U}(\hat{\Theta} + \mu I)^{-1}\hat{U}^T, \quad (3.4)$$

where $\hat{A}_N = \hat{U}\hat{\Theta}\hat{U}^T$ is a finite precision rank k Nyström approximation of A obtained via Algorithm 2.1 and $\hat{\lambda}_k$ is the smallest eigenvalue of \hat{A}_N . Columns of \hat{U} are the eigenvectors of \hat{A}_N computed in the working precision u and we thus assume that they are orthogonal. Then \hat{P}^{-1} is symmetric positive definite and it has $n - k$ eigenvalues equal to one and the rest are equal to $(\hat{\lambda}_k + \mu)/(\hat{\lambda}_i + \mu)$ for $i = 1, 2, \dots, k$, where $\hat{\lambda}_i > \hat{\lambda}_{i+1}$ are the nonzero eigenvalues of \hat{A}_N .

THEOREM 3.1. *Let $(A + \mu I) \in \mathbb{R}^{n \times n}$ be symmetric positive definite, \hat{P}^{-1} as defined in (3.4), and E and \mathcal{E} as defined in (2.1) and (2.3), respectively. The condition number $\kappa(\hat{P}^{-1/2}(A + \mu I)\hat{P}^{-1/2})$ can be bounded as*

$$\max \left\{ 1, \frac{\hat{\lambda}_k + \mu - \|\mathcal{E}\|_2}{\mu + \lambda_{\min}(A)} \right\} \leq \kappa(\hat{P}^{-1/2}(A + \mu I)\hat{P}^{-1/2}) \leq 1 + \frac{\hat{\lambda}_k + \|E\|_2 + 2\|\mathcal{E}\|_2}{\mu - \|\mathcal{E}\|_2}, \quad (3.5)$$

where the upper bound holds if $\mu > \|\mathcal{E}\|_2$. Regardless of this constraint, if A is positive definite, then

$$\kappa(\widehat{P}^{-1/2}(A + \mu I)\widehat{P}^{-1/2}) \leq \left(\widehat{\lambda}_k + \mu + \|E\|_2 + \|\mathcal{E}\|_2\right) \left(\frac{1}{\widehat{\lambda}_k + \mu} + \frac{\|\mathcal{E}\|_2 + 1}{\lambda_{\min}(A) + \mu}\right). \quad (3.6)$$

Proof. We first obtain the upper bounds for the condition number. Since $A = \widehat{A}_N + E + \mathcal{E}$, Weyl's inequality gives the bound

$$\begin{aligned} \lambda_{\max}(\widehat{P}^{-1/2}(A + \mu I)\widehat{P}^{-1/2}) &\leq \lambda_{\max}(\widehat{P}^{-1/2}(\widehat{A}_N + \mu I)\widehat{P}^{-1/2}) \\ &\quad + \lambda_{\max}(\widehat{P}^{-1/2}E\widehat{P}^{-1/2}) + \lambda_{\max}(\widehat{P}^{-1/2}\mathcal{E}\widehat{P}^{-1/2}). \end{aligned}$$

The eigenvalues $\lambda_{\max}(\widehat{P}^{-1/2}(\widehat{A}_N + \mu I)\widehat{P}^{-1/2})$ and $\lambda_{\max}(\widehat{P}^{-1/2}E\widehat{P}^{-1/2})$ can hence be bounded as in [10], because $\widehat{P}^{-1/2}$ is constructed with eigenpairs of \widehat{A}_N and E is positive semidefinite and thus $\widehat{P}^{-1/2}E\widehat{P}^{-1/2}$ is also positive semidefinite. We thus have

$$\lambda_{\max}(\widehat{P}^{-1/2}(\widehat{A}_N + \mu I)\widehat{P}^{-1/2}) + \lambda_{\max}(\widehat{P}^{-1/2}E\widehat{P}^{-1/2}) \leq \widehat{\lambda}_k + \mu + \|E\|_2. \quad (3.7)$$

Since we assume that \widehat{U} has orthogonal columns and thus $\sigma_{\max}(\widehat{P}^{-1}) = 1$ when $k < n$, we have

$$\begin{aligned} \lambda_{\max}(\widehat{P}^{-1/2}\mathcal{E}\widehat{P}^{-1/2}) &= \lambda_{\max}(\widehat{P}^{-1}\mathcal{E}) \\ &\leq \max_i |\lambda_i(\widehat{P}^{-1}\mathcal{E})| \\ &\leq \sigma_{\max}(\widehat{P}^{-1}\mathcal{E}) \\ &\leq \sigma_{\max}(\widehat{P}^{-1})\sigma_{\max}(\mathcal{E}) \\ &= \sigma_{\max}(\mathcal{E}) \\ &= \|\mathcal{E}\|_2. \end{aligned} \quad (3.8)$$

Combining (3.7) and (3.8) gives

$$\lambda_{\max}(\widehat{P}^{-1/2}(A + \mu I)\widehat{P}^{-1/2}) \leq \widehat{\lambda}_k + \mu + \|E\|_2 + \|\mathcal{E}\|_2. \quad (3.9)$$

We bound $\lambda_{\min}(\widehat{P}^{-1/2}(A + \mu I)\widehat{P}^{-1/2})$ using Weyl's inequality and the facts that we have $\lambda_{\min}(\widehat{P}^{-1/2}(\widehat{A}_N + \mu I)\widehat{P}^{-1/2}) \geq \mu$ and $\lambda_{\min}(\widehat{P}^{-1/2}E\widehat{P}^{-1/2}) \geq 0$ as follows:

$$\begin{aligned} \lambda_{\min}(\widehat{P}^{-1/2}(A + \mu I)\widehat{P}^{-1/2}) &\geq \lambda_{\min}(\widehat{P}^{-1/2}(\widehat{A}_N + \mu I)\widehat{P}^{-1/2}) \\ &\quad + \lambda_{\min}(\widehat{P}^{-1/2}E\widehat{P}^{-1/2}) + \lambda_{\min}(\widehat{P}^{-1/2}\mathcal{E}\widehat{P}^{-1/2}) \\ &\geq \mu + \lambda_{\min}(\widehat{P}^{-1/2}\mathcal{E}\widehat{P}^{-1/2}) \\ &\geq \mu - \|\mathcal{E}\|_2. \end{aligned} \quad (3.10)$$

Assuming that $\mu > \|\mathcal{E}\|_2$, from (3.9) and (3.10) we have

$$\kappa(\widehat{P}^{-1/2}(A + \mu I)\widehat{P}^{-1/2}) \leq \frac{\widehat{\lambda}_k + \mu + \|E\|_2 + \|\mathcal{E}\|_2}{\mu - \|\mathcal{E}\|_2} = 1 + \frac{\widehat{\lambda}_k + \|E\|_2 + 2\|\mathcal{E}\|_2}{\mu - \|\mathcal{E}\|_2},$$

which proves the upper bound in (3.5).

The condition $\mu > \|\mathcal{E}\|_2$ may not be satisfied for small values of μ . It can be avoided if A is positive definite. Following the argument in [10], we consider

$$\begin{aligned}\lambda_{\min} \left(\widehat{P}^{-1/2} (A + \mu I) \widehat{P}^{-1/2} \right) &= \lambda_{\min} \left((A + \mu I)^{1/2} \widehat{P}^{-1} (A + \mu I)^{1/2} \right) \\ &= \frac{1}{\lambda_{\max} \left((A + \mu I)^{-1/2} \widehat{P} (A + \mu I)^{-1/2} \right)}\end{aligned}\quad (3.11)$$

and bound $\lambda_{\max} \left((A + \mu I)^{-1/2} \widehat{P} (A + \mu I)^{-1/2} \right)$ from above. Using Weyl's inequality, we obtain

$$\begin{aligned}\lambda_{\max} \left((A + \mu I)^{-1/2} \widehat{P} (A + \mu I)^{-1/2} \right) &= \lambda_{\max} \left((A + \mu I)^{-1/2} \left(\frac{1}{\widehat{\lambda}_k + \mu} \left(\widehat{A}_N + \mu \widehat{U} \widehat{U}^T \right) + \left(I - \widehat{U} \widehat{U}^T \right) \right) (A + \mu I)^{-1/2} \right) \\ &\leq \frac{1}{\widehat{\lambda}_k + \mu} \lambda_{\max} \left((A + \mu I)^{-1/2} \left(\widehat{A}_N + \mu \widehat{U} \widehat{U}^T \right) (A + \mu I)^{-1/2} \right) \\ &\quad + \lambda_{\max} \left((A + \mu I)^{-1/2} \left(I - \widehat{U} \widehat{U}^T \right) (A + \mu I)^{-1/2} \right).\end{aligned}\quad (3.12)$$

$$(3.13)$$

To bound (3.12), we use Weyl's inequality again, giving

$$\begin{aligned}\lambda_{\max} \left((A + \mu I)^{-1/2} \left(\widehat{A}_N + \mu \widehat{U} \widehat{U}^T \right) (A + \mu I)^{-1/2} \right) &= \lambda_{\max} \left((A + \mu I)^{-1/2} \left(\widehat{A}_N + \mathcal{E} - \mathcal{E} + \mu \widehat{U} \widehat{U}^T \right) (A + \mu I)^{-1/2} \right) \\ &\leq \lambda_{\max} \left((A + \mu I)^{-1/2} \left(\widehat{A}_N + \mathcal{E} + \mu \widehat{U} \widehat{U}^T \right) (A + \mu I)^{-1/2} \right) \\ &\quad + \lambda_{\max} \left(-(A + \mu I)^{-1/2} \mathcal{E} (A + \mu I)^{-1/2} \right).\end{aligned}$$

Note that $\widehat{A}_N + \mathcal{E} = A_N$ is the Nyström approximation of A in infinite precision and thus $A - A_N$ is positive semidefinite. Then

$$(A + \mu I) - (\widehat{A}_N + \mathcal{E} + \mu \widehat{U} \widehat{U}^T) = A - A_N + \mu(I - \widehat{U} \widehat{U}^T)$$

is also positive semidefinite, because $I - \widehat{U} \widehat{U}^T$ is an orthogonal projector. Hence $I - (A + \mu I)^{-1}(\widehat{A}_N + \mathcal{E} + \mu \widehat{U} \widehat{U}^T)$ is positive semidefinite and by [19, Section 7.7]

$$\lambda_{\max} \left((A + \mu I)^{-1/2} \left(\widehat{A}_N + \mathcal{E} + \mu \widehat{U} \widehat{U}^T \right) (A + \mu I)^{-1/2} \right) \leq 1. \quad (3.14)$$

Further,

$$\begin{aligned}\lambda_{\max} \left(-(A + \mu I)^{-1/2} \mathcal{E} (A + \mu I)^{-1/2} \right) &\leq \max_i \left| \lambda_i \left((A + \mu I)^{-1/2} \mathcal{E} (A + \mu I)^{-1/2} \right) \right| \\ &= \max_i \left| \lambda_i \left((A + \mu I)^{-1} \mathcal{E} \right) \right| \\ &\leq \sigma_{\max} \left((A + \mu I)^{-1} \mathcal{E} \right) \\ &\leq \|(A + \mu I)^{-1}\|_2 \|\mathcal{E}\|_2 \\ &= \frac{\|\mathcal{E}\|_2}{\lambda_{\min}(A) + \mu}.\end{aligned}\quad (3.15)$$

The term in (3.13) is bounded as in [10], because $I - \widehat{U}\widehat{U}^T$ is an orthogonal projector and $\|I - \widehat{U}\widehat{U}^T\|_2 = 1$, that is,

$$\lambda_{max} \left((A + \mu I)^{-1/2} \left(I - \widehat{U}\widehat{U}^T \right) (A + \mu I)^{-1/2} \right) \leq \frac{1}{\lambda_{min}(A) + \mu}. \quad (3.16)$$

From (3.14), (3.15), and (3.16), we obtain

$$\lambda_{max} \left((A + \mu I)^{-1/2} \widehat{P} (A + \mu I)^{-1/2} \right) \leq \frac{1}{\widehat{\lambda}_k + \mu} + \frac{\|\mathcal{E}\|_2 + 1}{\lambda_{min}(A) + \mu} \quad (3.17)$$

and thus combining (3.17), (3.11), and (3.9), we have

$$\kappa(\widehat{P}^{-1/2}(A + \mu I)\widehat{P}^{-1/2}) \leq \left(\widehat{\lambda}_k + \mu + \|E\|_2 + \|\mathcal{E}\|_2 \right) \left(\frac{1}{\widehat{\lambda}_k + \mu} + \frac{\|\mathcal{E}\|_2 + 1}{\lambda_{min}(A) + \mu} \right),$$

which proves (3.6).

We now obtain the lower bound for the condition number in (3.5). The lower bound for $\lambda_{max}(\widehat{P}^{-1/2}(A + \mu I)\widehat{P}^{-1/2})$ is acquired using the same ideas as for $\lambda_{min}(\widehat{P}^{-1/2}(A + \mu I)\widehat{P}^{-1/2})$ above, that is,

$$\begin{aligned} \lambda_{max}(\widehat{P}^{-1/2}(A + \mu I)\widehat{P}^{-1/2}) &\geq \lambda_{max}(\widehat{P}^{-1/2}(\widehat{A}_N + \mu I + E)\widehat{P}^{-1/2}) \\ &\quad + \lambda_{min}(\widehat{P}^{-1/2}\mathcal{E}\widehat{P}^{-1/2}) \\ &\geq \lambda_{max}(\widehat{P}^{-1/2}(\widehat{A}_N + \mu I)\widehat{P}^{-1/2}) + \lambda_{min}(\widehat{P}^{-1/2}E\widehat{P}^{-1/2}) \\ &\quad + \lambda_{min}(\widehat{P}^{-1/2}\mathcal{E}\widehat{P}^{-1/2}) \\ &\geq \widehat{\lambda}_k + \mu - \|\mathcal{E}\|_2. \end{aligned}$$

The upper bound for $\lambda_{min}(\widehat{P}^{-1/2}(A + \mu I)\widehat{P}^{-1/2}) = \lambda_{min}((A + \mu I)\widehat{P}^{-1})$ is obtained as in [10], namely

$$\lambda_{min}((A + \mu I)\widehat{P}^{-1}) \leq \lambda_{min}(A + \mu I)\lambda_{max}(\widehat{P}^{-1}) = \lambda_{min}(A) + \mu.$$

We thus have

$$\kappa(\widehat{P}^{-1/2}(A + \mu I)\widehat{P}^{-1/2}) \geq \max \left\{ 1, \frac{\widehat{\lambda}_k + \mu - \|\mathcal{E}\|_2}{\mu + \lambda_{min}(A)} \right\},$$

because the condition number is always at least 1. \square

If $\|\mathcal{E}\|_2 = 0$, then the bounds in Theorem 3.1 coincide with the bounds in [10]. The lower bound is useful when $\widehat{\lambda}_k + \mu - \|\mathcal{E}\|_2 > \mu + \lambda_{min}(A)$, that is, when $\widehat{\lambda}_k > \|\mathcal{E}\|_2 + \lambda_{min}(A)$, which can be expected to hold when large eigenvalues are approximated. The finite precision error has an additive effect on the bounds and expands them, and a multiplicative effect appears in (3.6) for the case of SPD A .

4. Numerical examples. We illustrate the theory with simple numerical experiments in MATLAB R2020a. The Nyström approximation is constructed setting u_p to double, single, and half precision. Single and half precisions are simulated using the *chop* function [17]. The working precision u is set to double. An ‘exact’ Nyström approximation is computed using the Advanpix Multiprecision Computing Toolbox [2] at 64 decimal digits precision for all computations in Algorithm 2.1. The same

extended precision is used to compute the total approximation error and \mathcal{E} , condition numbers, and all the bounds. Each experiment is performed ten times for every set of parameters: we generate G in Algorithm 2.1 using MATLAB *randn* function with random seed set to values $\{1, 2, \dots, 10\}$, and report the means. There is no oversampling.

We explore the approximation problem without preconditioning and consider synthetic and application problems in section 4.1. The approximations of A are used to construct the LMP and the preconditioned shifted systems are solved via PCG in section 4.2. Experiments using quarter precision are presented in section 4.3.

4.1. Low-rank approximation. We compute the L_2 norms of the finite precision error \mathcal{E} and the total approximation error $A - \hat{A}_N$. The finite precision error is compared to

$$n^{3/2} \tilde{\gamma}_n^{(p)} \|A\|_2 \quad (4.1)$$

with $c = 1$.

4.1.1. Synthetic problems. We perform experiments with synthetic matrices described in [28]. $A \in \mathbb{R}^{n \times n}$ is a real matrix with effective rank r and is constructed in the following ways.

- *Exponential decay:*

$$A = \text{diag}(\beta_1, \beta_2, \dots, \beta_r, 10^{-q}, 10^{-2q}, \dots, 10^{-(n-r)q}),$$

where q is set to values 0.1, 0.25, and 1.

- *Polynomial decay:*

$$A = \text{diag}(\beta_1, \beta_2, \dots, \beta_r, 2^{-p}, 3^{-p}, \dots, (n-r+1)^{-p}),$$

where p is set to 0.5, 1, and 2.

- *PSD noise:*

$$A = \text{diag}(\beta_1, \beta_2, \dots, \beta_r, 0, \dots, 0) + \xi n^{-1} (GG^T),$$

where $G \in \mathbb{R}^{n \times n}$ is a random Gaussian matrix, and ξ is set to 10^{-4} , 10^{-2} , and 10^{-1} with higher values corresponding to greater noise.

We set $n = 10^2$, $r = 10$, $\beta_1 = \beta_2 = \dots = \beta_r =: \beta$. Values of β span $1, 10, 10^2, \dots, 10^{16}$. Note that $\|A\|_2 = \beta$ in the exponential and polynomial decay examples, and $\|A\|_2$ is well approximated by β in the PSD noise case. Experiments with half precision are performed when $\|A\|_2 < 10^5$. We compute rank $k \in \{1, 2, \dots, 10\}$ approximations.

We report the computed total and finite precision error in Figure 4.1 for the polynomial decay problem with $p = 1$; the results are similar for all the synthetic problems. Recall that our finite error analysis assumes $\Delta \leq 1$. In these experiments, this condition can be violated for some k when $\|A\|_2 > 10^3$ and u_p is set to half precision, and $\|A\|_2 > 10^7$ and u_p is set to single precision. Despite this condition being violated, we can see that the measured finite precision error is still less than (4.1).

When $k < 10$, E is dominated by $\beta_{k+1}, \beta_{k+2}, \dots, \beta_r$ and the finite precision error \mathcal{E} stays significantly smaller. When $k = 10$, all the large eigenvalues are being approximated and the exact approximation error E depends on the small eigenvalues. The finite precision error thus becomes important and affects the approximation quality detrimentally for large $\|A\|_2$.

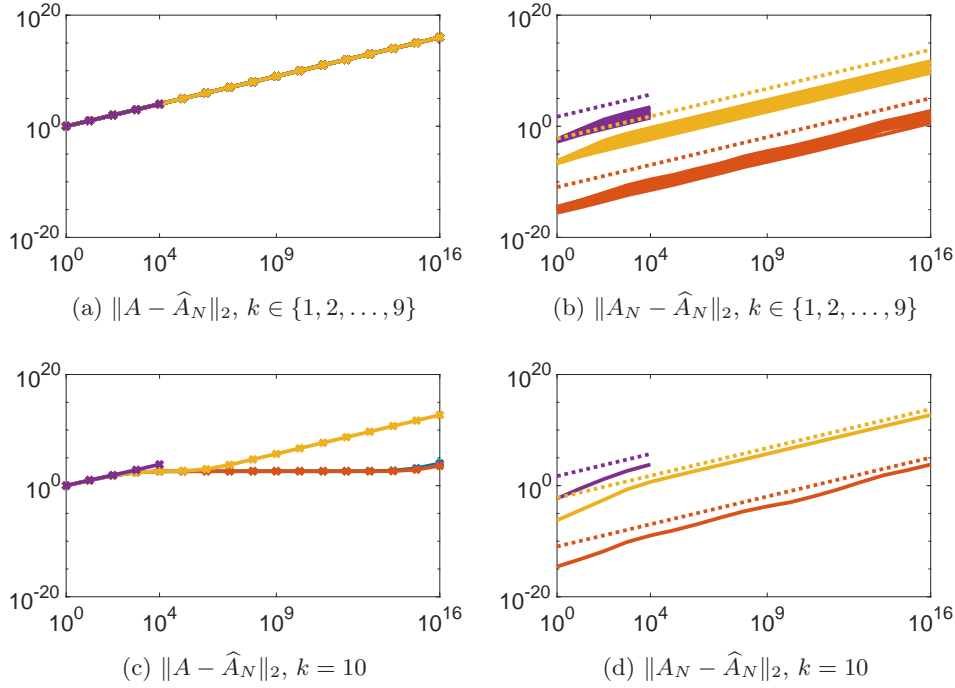


Fig. 4.1: Polynomial decay problem with $p = 1$. The left panels show the L_2 norms of the mean total error $A - \widehat{A}_N$ (crossed) and the right panels show the L_2 norms of the mean finite precision error $A_N - \widehat{A}_N$ (solid) for every k value versus $\|A\|_2$. The precision u_p is set to half (purple), single (yellow), double (red), and ‘exact’ (blue). The finite precision error is estimated by (4.1) (dotted). When $k < 10$ the total error is indistinguishable for all precisions.

4.1.2. SuiteSparse problems. We now consider some symmetric positive definite problems from the SuiteSparse matrix collection [8]. Their properties are summarised in Table 4.1. The problems have different spectral properties including the decay of the largest eigenvalues and spectral gaps. The normalised spectra $\lambda_{k+1}/\lambda_{max}$ and $\sqrt{n}u_p$ to estimate when the finite precision error becomes significant (as in (2.8)) are shown in Figure 4.2 when u_p is set to single and half precision.

We report the total and finite precision errors in Figures 4.3 and 4.4 for various k values. The k values are chosen so that we approximate eigenvalues throughout different parts of the spectrum; if there is a relatively large gap between eigenvalues λ_j and λ_{j+1} , then we test $k = j$ and $k = j+1$. Note that this results in the nonuniform spacing of the x -axes in Figures 4.3 and 4.4.

The finite precision error $\|\mathcal{E}\|_2$ is bounded by (4.1) with the values given in Table 4.2. The error due to low precision affects the quality of the approximation when $\|E\|_2 \approx \|\mathcal{E}\|_2$, which is the case for relatively large k values, and is not observed with $k \leq 130$ for the bcsstk22 problem. The heuristic (2.8) gives a good estimate of when this happens (Figure 4.2). The finite precision error increases when eigenvalues close to a spectral gap are approximated.

| Problem | n | $\ A\ _2$ | half precision |
|----------|-----|-----------------------|----------------|
| Journals | 124 | 6.85×10^4 | yes |
| bcsstm07 | 420 | 2.51×10^3 | yes |
| plat362 | 362 | 7.74×10^{-1} | yes |
| 494_bus | 494 | 3.00×10^4 | yes |
| nos7 | 729 | 9.86×10^6 | no |
| bcsstk22 | 138 | 5.85×10^6 | no |
| LFAT5 | 14 | 2.15×10^7 | no |

Table 4.1: Problems from the SuiteSparse collection [8], where A is an $n \times n$ positive definite matrix. Half precision is used for problems where the largest eigenvalues belong to the range of half precision, see Table 1.1.

| Problem | u_p | | |
|----------|------------------------|-----------------------|--------------------|
| | double | single | half |
| Journals | 1.30×10^{-6} | 7.00×10^2 | 6.10×10^6 |
| bcsstm07 | 1.01×10^{-6} | 5.41×10^2 | 5.57×10^6 |
| plat362 | 2.14×10^{-10} | 1.15×10^{-1} | 1.15×10^3 |
| 494_bus | 1.81×10^{-5} | 9.70×10^3 | 1.05×10^8 |
| nos7 | 1.57×10^{-2} | 8.44×10^6 | - |
| bcsstk22 | 1.45×10^{-4} | 7.80×10^4 | - |
| LFAT5 | 1.75×10^{-6} | 9.38×10^2 | - |

Table 4.2: Finite precision error bound (4.1) for the problems in Table 4.1.

4.2. Preconditioned systems. We are interested in comparing the preconditioning performance for shifted systems (3.1) when the preconditioner (3.4) is constructed using an approximation computed via Algorithm 2.1 with different precisions u_p . This is done by computing the condition number of preconditioned systems and solving them via PCG in double precision. We consider problems from the SuiteSparse collection described in the previous section, except plat362 for which the preconditioning with (3.4) is not expected to be useful, because all eigenvalues of A are smaller than one. We consider the same k values as in the previous section and refer the reader to [10] for strategies on choosing an optimal k . Note that the computational cost of generating the preconditioner depends on the precision u_p , but the cost of applying the preconditioner does not.

4.2.1. Condition number. We compute the condition number of split-preconditioned matrices

$$\widehat{P}^{-1/2}(A + \mu I)\widehat{P}^{-1/2},$$

where $\widehat{P}^{-1/2}$ is constructed as in defined in (3.4).

To simplify notation, we denote the quantities in the condition number bounds

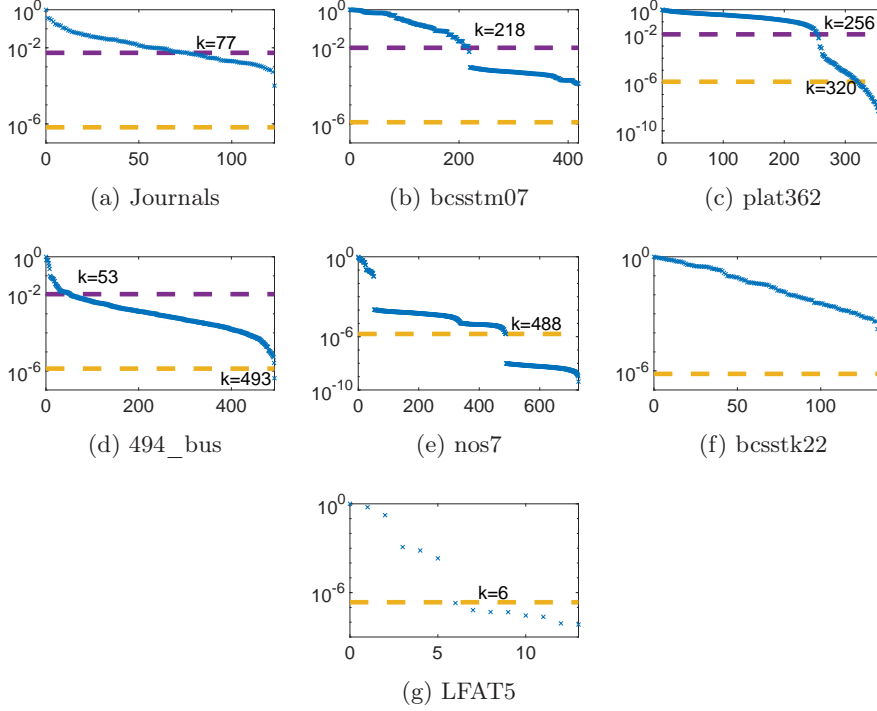


Fig. 4.2: Normalised spectra $\lambda_{k+1}/\lambda_{max}$ (blue crosses) versus k , and $\sqrt{n}u_p$ (dashed) for the problems in Table 4.1 with text indicating the point of intersection. For the dashed lines, colours indicating single (yellow) and half (purple) precision are the same as in Figure 4.1.

in Theorem 3.1 as follows:

$$\begin{aligned}
 b_{\text{low}} &= \max \left\{ 1, \frac{\widehat{\lambda}_k + \mu - \|\mathcal{E}\|_2}{\mu + \lambda_{\min}(A)} \right\}, \\
 b_{\text{upp}} &= 1 + \frac{\widehat{\lambda}_k + \|E\|_2 + 2\|\mathcal{E}\|_2}{\mu - \|\mathcal{E}\|_2}, \\
 b_{\text{uppspd}} &= \left(\widehat{\lambda}_k + \mu + \|E\|_2 + \|\mathcal{E}\|_2 \right) \left(\frac{1}{\widehat{\lambda}_k + \mu} + \frac{\|\mathcal{E}\|_2 + 1}{\lambda_{\min}(A) + \mu} \right).
 \end{aligned}$$

We compute approximations of these quantities by replacing $\|E\|_2$ with the expected error $\mathbb{E}\|E\|_2$ in (2.2) and $\|\mathcal{E}\|_2$ with the bound (4.1). We set μ to 0, 0.1, 0.5 and 1. Thus b_{upp} is only computed when u_p is set to double precision for all problems.

We report results for $\mu = 0.5$ in Figure 4.5; the results for different μ values are similar. The mean condition numbers are bounded by the mean estimated bounds and the preconditioning reduces the condition number when an appropriate k is chosen. There is very little difference in the condition number regardless of the precision and it arises when there is a difference in the total approximation error. The estimated bounds however get worse with lower precision. The lower bound for half precision for all the problems and single precision for 494_bus and nos7 problems or large k

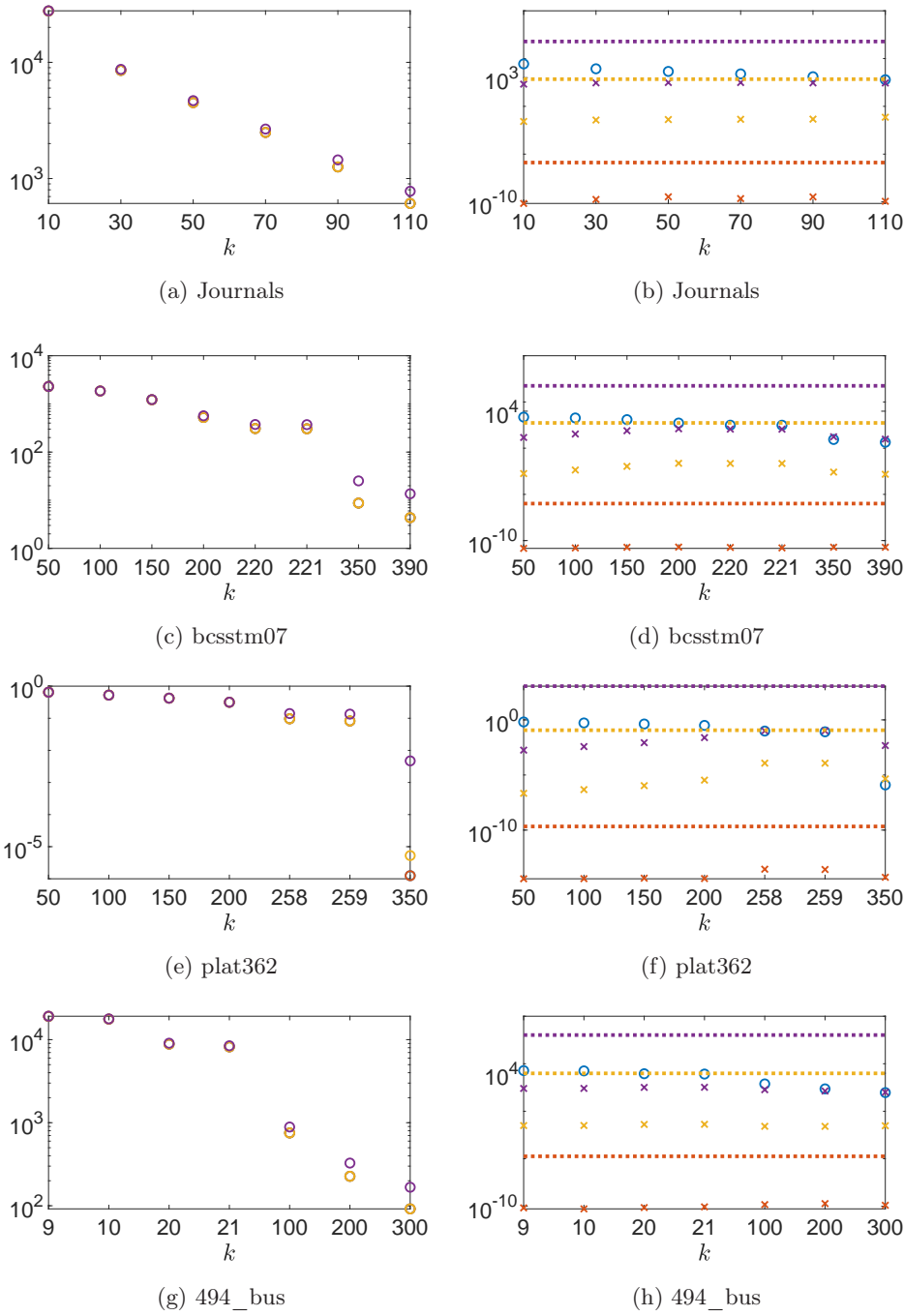


Fig. 4.3: SuiteSparse problems. The left panels show L_2 norms of the mean total error $\|A - \hat{A}_N\|_2$ (circles). The right panels show the mean finite precision error $\|A_N - \hat{A}_N\|_2$ (crosses), the mean exact approximation error $\|A - A_N\|_2$ (blue circles), and estimates of the finite precision error (dashed lines) versus the rank of approximation k . In both panels, u_p is indicated by the colour of the markers: purple denotes half, yellow denotes single, and red denotes double.

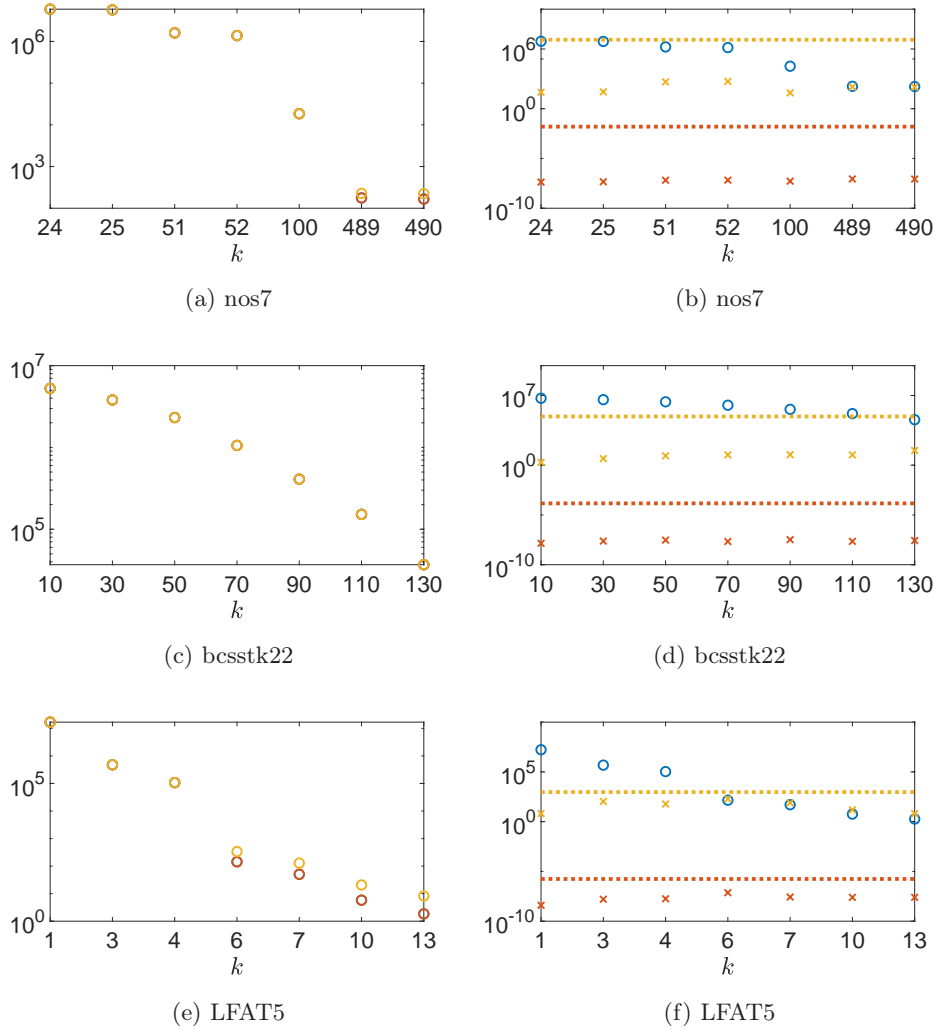


Fig. 4.4: SuiteSparse problems where half precision is not used. Left panels show L_2 norms of the mean total error $\|A - \widehat{A}_N\|_2$ (circles). Right panels show the mean finite precision error $\|A_N - \widehat{A}_N\|_2$ (crosses), the mean exact approximation error $\|A - A_N\|_2$ (blue circles), and estimates of the finite precision error (dashed lines) versus rank k . In both panels, u_p is indicated by the marker colour: yellow denotes single and red denotes double.

values is equal to one and thus not useful. b_{upp} and b_{uppspd} either coincide or are very similar, except for the Journals and bcsstk22 problems.

4.2.2. Solving the systems. We now solve the systems in (3.1) with PCG with left-preconditioning, that is,

$$\widehat{P}^{-1}(A + \mu I)x = \widehat{P}^{-1}b.$$

\widehat{P}^{-1} is constructed as in the previous section. The entries of b are uniformly distributed random numbers where the random number generator seed is set to 1234.

The mean iteration count results in Figure 4.6 correspond to the condition number results in Figure 4.5. There is very little, if any, observable difference in PCG iteration count when the preconditioner is constructed in different precisions, even for large k values. This indicates that in many practical cases, the mixed precision Nyström method is likely suitable for use in generating preconditioners for PCG.

4.3. Quarter precision. Given the recent availability of quarter precision (fp8) on the NVIDIA H100 GPUs, we briefly explore its use in the mixed precision single-pass Nyström method. NVIDIA offers two variants of fp8 arithmetic: fp8-e5m2, which has 5 exponent bits and 2 significand bits, and fp8-e4m3, which has 4 exponent bits and 3 significand bits [4]. The format fp8-e5m2 has the same range as half precision and unit roundoff $u = 2^{-2} = 0.25$ and fp8-e4m3 has a smaller range and unit roundoff $u = 2^{-3} = 0.125$. We perform experiments with Journals, bcsstm07, plat362, and 494_bus problems setting u_p to fp8-e5m2 and fp8-e4m3 precisions which are simulated with *chop* function [17]. Note that our theoretical analysis does not hold, because $nu_p > 1$.

Using fp8-e4m3 results in overflow or underflow with $k = 1$ for all problems except plat362. For this problem, the total approximation error is not affected by using both quarter precisions with $k = 50$, but is detrimental with larger k values (not shown). Results for the Journals and bcsstm07 problems when small rank k approximations are generated with u_p set to fp8-e5m2 are reported in Figure 4.7. From the top row of plots it is clear that the total approximation error is dominated by the finite precision error. Even though the condition number of the preconditioned coefficient matrix is generally smaller than in the unpreconditioned case (middle row), the preconditioner either accelerates the convergence only slightly (Journals) or affects it detrimentally (bcsstm07) (bottom row). The preconditioner is not useful with large k values and the 494_bus problem (not shown). Our results suggest that further work to evaluate the suitability of fp8 arithmetic in this context is needed; in particular, sophisticated scaling techniques as in [18] may be useful for improving the behavior of computations in fp8-e4m3.

5. Conclusions. In this paper, we considered a mixed precision variant of the single-pass Nyström method for approximating an SPD matrix A , where the expensive products with A are performed in lower precision than the other computations. We bound the total approximation error taking into account the lower precision. A good quality approximation is obtained when the finite precision error is smaller than the error of the exact Nyström approximation itself. This corresponds to the case when only relatively large eigenvalues are approximated. Numerical examples with both synthetic problems and applications problems confirm this observation.

We also analysed a randomised limited memory preconditioner constructed with the mixed precision Nyström approximation. We proved bounds on the condition number of the preconditioned coefficient matrix which take into account the low precision error. The preconditioner is of most interest when it is constructed with a relatively low rank approximation, and in this case using the low precision for products with A does not diminish the quality of the preconditioner in terms of resulting iterations of the conjugate gradient method.

The limited range of the low precision restricts the extent of problems that can be considered in the mixed precision framework. This is problematic if setting the low precision to quarter or half is desired. An algorithm that maps matrix to half precision

sion and preserves symmetry is proposed by [18]. Future work on developing scaling algorithms that preserve the positive semidefiniteness property and the structure of the spectrum is of high interest.

REFERENCES

- [1] A. ABDELFAH, H. ANZT, E. G. BOMAN, E. CARSON, T. COJEAN, J. DONGARRA, A. FOX, M. GATES, N. J. HIGHAM, X. S. LI, ET AL., *A survey of numerical linear algebra methods utilizing mixed-precision arithmetic*, Int. J. High Perf. Comput. Appl., 35 (2021), pp. 344–369.
- [2] *Advantix multiprecision computing toolbox for MATLAB*. <http://www.advantix.com>.
- [3] H. AL DAAS, T. REES, AND J. SCOTT, *Two-level Nyström-Schur preconditioner for sparse symmetric positive definite matrices*, SIAM J. Sci. Comput., 43 (2021), pp. A3837 – A3861.
- [4] M. ANDERSCH, G. PALMER, R. KRASHINSKY, N. STAM, V. MEHTA, G. BRITO, AND S. RAMASWAMY, *NVIDIA Hopper architecture in-depth*. <https://developer.nvidia.com/blog/nvidia-hopper-architecture-in-depth>.
- [5] E. CARSON AND Z. STRAKOŠ, *On the cost of iterative computations*, Phil. Trans. Royal Soc. A: Math., Phys. and Eng. Sci., 378 (2020), p. 20190050.
- [6] I. DAUZICKAITĖ, A. S. LAWLESS, J. A. SCOTT, AND P. J. VAN LEEUWEN, *Randomised preconditioning for the forcing formulation of weak constraint 4D-Var*, Quarterly J. Royal Met. Soc., 147 (2021), pp. 3719 – 3734.
- [7] K. R. DAVIDSON AND S. J. SZAREK, *Chapter 8 - local operator theory, random matrices and Banach spaces*, in Handbook of the Geometry of Banach Spaces, W. Johnson and J. Lindenstrauss, eds., vol. 1 of Handbook of the Geometry of Banach Spaces, Elsevier Science B.V., 2001, pp. 317 – 366.
- [8] T. A. DAVIS AND Y. HU, *The University of Florida sparse matrix collection*, ACM Trans. Math. Softw., 38 (2011), <https://doi.org/10.1145/2049662.2049663>.
- [9] P. DRINEAS AND M. W. MAHONEY, *On the Nyström method for approximating a Gram matrix for improved kernel-based learning*, J. Mach. Learn. Res., 6 (2005), pp. 2153 – 2175.
- [10] Z. FRANGELLA, J. A. TROPP, AND M. UDELL, *Randomized Nyström preconditioning*, arXiv preprint arXiv:2110.02820, (2021).
- [11] L. GIRAUD AND S. GRATTON, *On the sensitivity of some spectral preconditioners*, SIAM J. Matrix Anal. Appl., 27 (2006), pp. 1089 – 1105.
- [12] A. GITTENS, *Topics in randomized numerical linear algebra*, PhD thesis, California Institute of Technology, 2013.
- [13] A. GITTENS AND M. W. MAHONEY, *Revisiting the Nyström method for improved large-scale machine learning*, J. Mach. Learn. Res., 17 (2016), pp. 3977 – 4041.
- [14] S. GRATTON, A. SARTENAER, AND J. TSHIMANGA, *On a class of limited memory preconditioners for large scale linear systems with multiple right-hand sides*, SIAM J. Opt., 21 (2011), pp. 912 – 935.
- [15] N. HALKO, P. MARTINSSON, AND J. TROPP, *Finding structure with randomness: Probabilistic algorithms for constructing approximate matrix decompositions*, SIAM Rev., 53 (2011), pp. 217 – 288.
- [16] N. J. HIGHAM, *Accuracy and Stability of Numerical Algorithms, 2nd Edition*, SIAM, Philadelphia, PA, 2002.
- [17] N. J. HIGHAM AND S. PRANESH, *Simulating low precision floating-point arithmetic*, SIAM J. Sci. Comput., 41 (2019), pp. C585 – C602.
- [18] N. J. HIGHAM, S. PRANESH, AND M. ZOUNON, *Squeezing a matrix into half precision, with an application to solving linear systems*, SIAM J. Sci. Comput., 41 (2019), pp. A2536 – A2551.
- [19] R. A. HORN AND C. R. JOHNSON, *Matrix Analysis*, Cambridge Univ. Press, Cambridge, UK, 2 ed., 2012.
- [20] P. LALOYLAUX, S. FROLOV, B. MÉNÉTRIÉ, AND M. BONAVIDA, *Implicit and explicit cross-correlations in coupled data assimilation*, Quarterly J. Royal Met. Soc., 144 (2018), pp. 1851 – 1863.
- [21] M. W. MAHONEY, *Randomized algorithms for matrices and data*, Found. Trends Mach. Learn., 3 (2011), pp. 123 – 224.
- [22] P. G. MARTINSSON AND J. A. TROPP, *Randomized numerical linear algebra: Foundations and algorithms*, Acta Numerica, 29 (2020), pp. 403 – 572.
- [23] K. MOGENSEN, M. ALONSO BALMASEDA, AND A. WEAVER, *The NEMOVAR ocean data assimilation system as implemented in the ECMWF ocean analysis for System 4*, ECMWF

- Technical Memoranda, (2012), p. 59.
- [24] A. M. MOORE, H. G. ARANGO, G. BROQUET, B. S. POWELL, A. T. WEAVER, AND J. ZAVALA-GARAY, *The regional ocean modeling system (ROMS) 4-dimensional variational data assimilation systems: Part I - system overview and formulation*, Prog. Oceanog., 91 (2011), pp. 34 – 49.
 - [25] Y. NAKATSUKASA, *Fast and stable randomized low-rank matrix approximation*, arXiv preprint arXiv:2009.11392, (2020).
 - [26] M. RUDELSON AND R. VERSHYNIN, *The least singular value of a random square matrix is $O(n^{-1/2})$* , Comptes Rendus Mathematique, 346 (2008), pp. 893 – 896.
 - [27] Y. SAAD, *Iterative Methods for Sparse Linear Systems*, SIAM, Philadelphia, PA, 2nd ed., 2003.
 - [28] J. A. TROPP, A. YURTSEVER, M. UDELL, AND V. CEVHER, *Fixed-rank approximation of a positive-semidefinite matrix from streaming data*, arXiv preprint arXiv:1706.05736, (2017).
 - [29] J. A. TROPP, A. YURTSEVER, M. UDELL, AND V. CEVHER, *Streaming low-rank matrix approximation with an application to scientific simulation*, SIAM J. Sci. Comput., 41 (2019), pp. A2430 – A2463.
 - [30] J. TSHIMANGA, *On a Class of Limited Memory Preconditioners for Large-Scale Nonlinear Least-Squares Problems (with Application to Variational Ocean Data Assimilation)*, PhD thesis, Department of Mathematics, University of Namur, Belgium, 2007.
 - [31] J. TSHIMANGA, S. GRATTON, A. T. WEAVER, AND A. SARTENAER, *Limited-memory preconditioners, with application to incremental four-dimensional variational data assimilation*, Quarterly J. Royal Met. Soc., 134 (2008), pp. 751 – 769.
 - [32] C. WILLIAMS AND M. SEEGER, *Using the Nyström method to speed up kernel machines*, in Advances in Neural Information Processing Systems, T. Leen, T. Dietterich, and V. Tresp, eds., vol. 13, MIT Press, 2000.

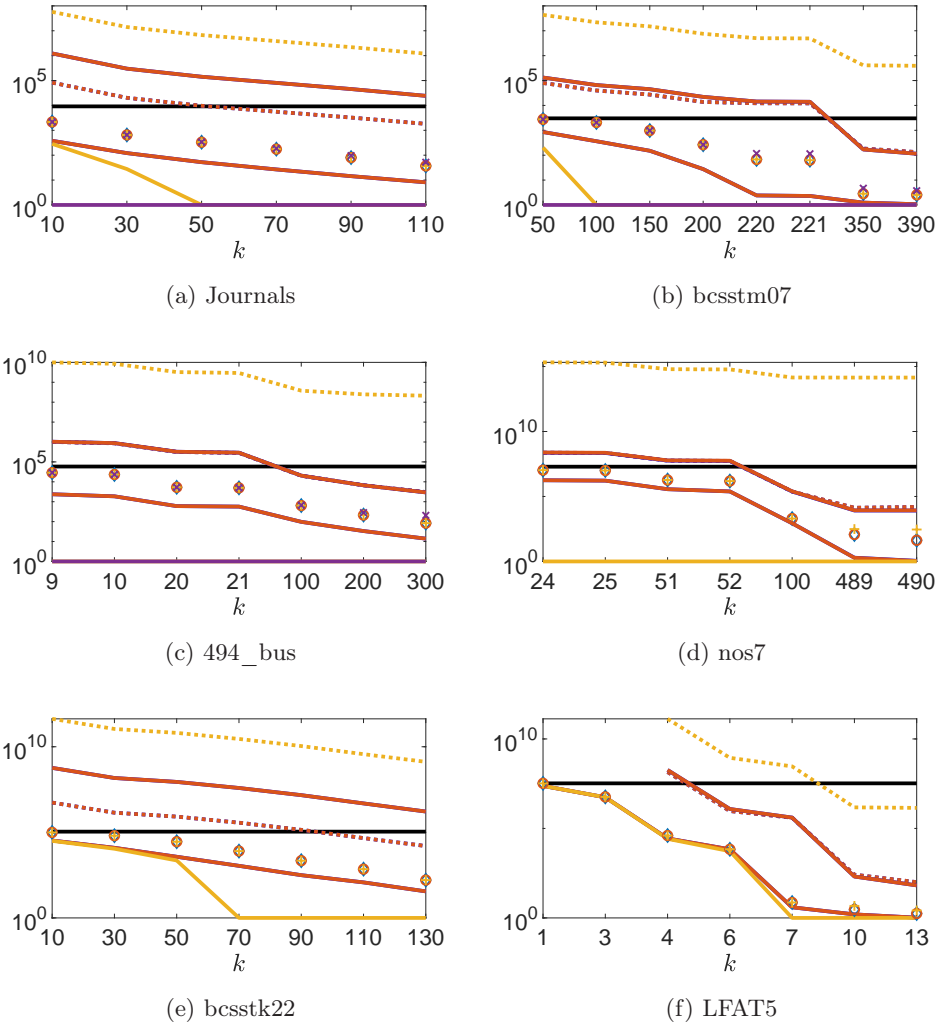


Fig. 4.5: Condition number of $A + 0.5I$ (black solid line) and the mean condition number of $\widehat{P}^{-1/2}(A + \mu I)\widehat{P}^{-1/2}$ (markers) with preconditioner (3.3) constructed using a rank k Nyström approximation. The mean estimates of the bounds b_{low} (solid), b_{upp} (solid; double only) and b_{uppspd} (dotted). The bounds b_{uppspd} with half precision are $O(10^{12})$ for the Journals problem, $O(10^{13})$ for bcsstm07, and $O(10^{17}) - O(10^{16})$ for 494_bus (not shown). The precision u_p is indicated by the colour and the type of the markers: purple crosses denote half, yellow pluses denote single, red circles denote double, and blue diamonds denote ‘exact’.

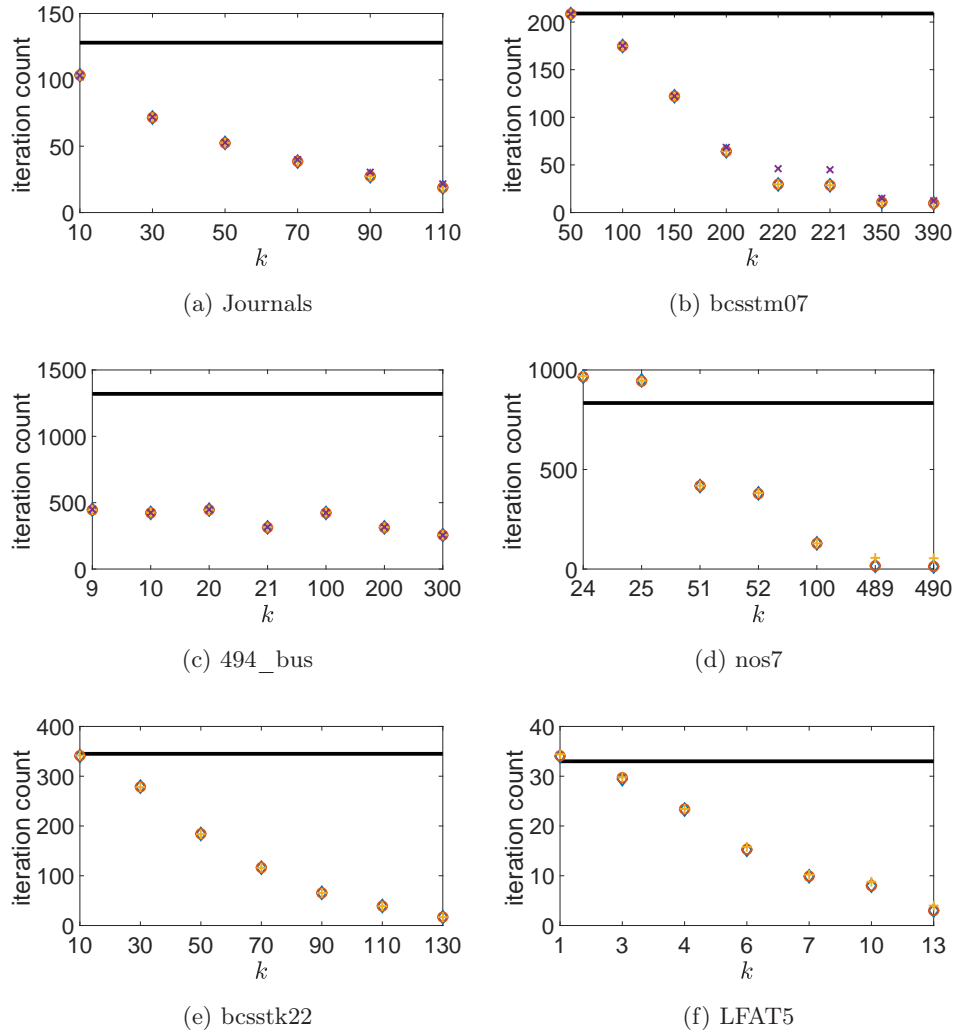


Fig. 4.6: Mean PCG iteration count when solving $(A + 0.5I)x = b$ without preconditioning (black) and with preconditioner (3.3) constructed using a rank k Nyström approximation (markers). The precision u_p is indicated by the colour and the type of the markers: purple crosses denote half, yellow pluses denote single, red circles denote double, and blue diamonds denote ‘exact’.

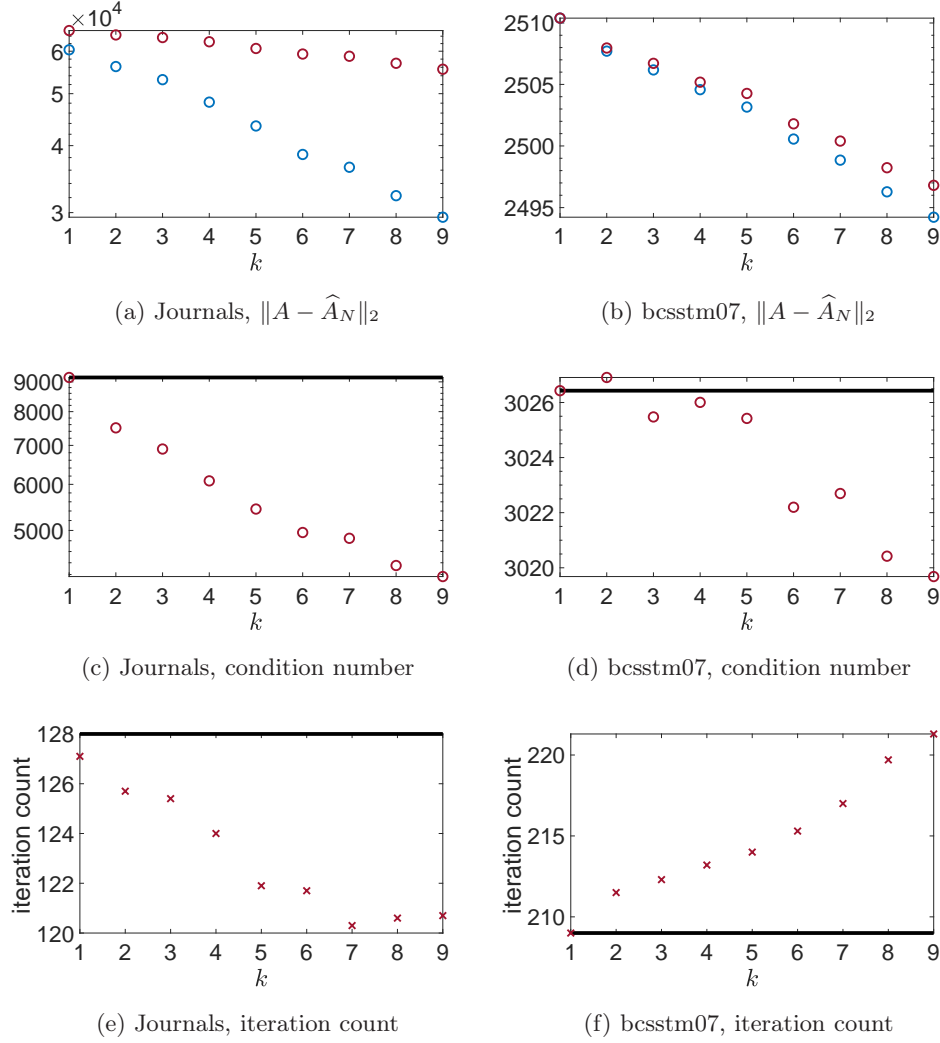


Fig. 4.7: u_p set to fp8-e5m2. The top panels show the total approximation error $\|A - \widehat{A}_N\|_2$ for the ‘exact’ approximation, i.e., $\|A - \widehat{A}_N\|_2 = \|A - A_N\|_2$ (blue circles), and the mixed precision approximation with u_p set to fp8-e5m2 (red circles) versus rank k . The middle panels show the condition number of $A + 0.5I$ (black) and $\widehat{P}^{-1/2}(A + \mu I)\widehat{P}^{-1/2}$ (red circles). The bottom panels show the mean PCG iteration count when solving $(A + 0.5I)x = b$ without preconditioning (black) and with preconditioner (3.4) (red crosses).